

Microhydration of the metastable *N*-Protomer of 4-Aminobenzoic acid by condensation at 80 K: H/D exchange without conversion to the more stable *O*-protomer

Thien Khuu,^a Santino J. Stropoli,^a Kim Greis,^{a,b} Nan Yang,^a and Mark A. Johnson^{a,*}

^a Sterling Chemistry Laboratory, Yale University, New Haven, CT, 06520

^b Institut für Chemie und Biochemie, Freie Universität Berlin, Arnimallee 22, 14195 Berlin (Germany);
Fritz-Haber-Institut der Max-Planck-Gesellschaft, Faradayweg 4–6, 14195 Berlin (Germany)

* Corresponding Author

Mark A. Johnson Email: mark.johnson@yale.edu

Keywords: 4-Aminobenzoic acid, *para*-Aminobenzoic acid, vibrational spectroscopy, protomer, isomer-selective

Abstract

4-Aminobenzoic acid (4ABA) is a model scaffold for studying solvent-mediated proton transfer. Although protonation at the carboxylic group (*O*-protomer) is energetically favored in the gas phase, the *N*-protomer, where the proton remains on the amino group, can be kinetically trapped by electrospray ionization of 4ABA in an aprotic solvent such as acetonitrile. Here we report the formation of the hydrated deuterium isotopologues of the *N*-protomers, $\text{RND}_3^+(\text{H}_2\text{O})_{n=1-3}$, ($\text{R}=\text{C}_6\text{H}_4\text{COOD}$), which are generated by condensing water molecules onto the bare *N*-protomers in a liquid nitrogen cooled, radiofrequency octopole ion trap at 80 K. The product clusters are then transferred to a 20 K cryogenic ion trap where they are tagged with weakly bound D_2 molecules. The structures of these clusters are determined by analysis of their vibrational patterns obtained by resonant IR photodissociation. The resulting patterns confirm that the metastable *N*-protomer configuration remains intact even when warmed by sequential condensation of water molecules. Attachment of H_2O molecules onto the RND_3^+ head group also affords the opportunity to explore the possibility of H/D exchange between the acid scaffold and the proximal water network. The spectroscopic results establish that although the $\text{RND}_3^+(\text{H}_2\text{O})_{n=1,2}$ clusters are formed without H/D exchange, the $n = 3$ cluster exhibits about 10% H/D exchange as evidenced by the appearance of the telltale HOD bands. The site of exchange on the acid is determined to be the acidic OH by the emergence of the OH stretching fundamental in the $-\text{COOH}$ motif.

I. Introduction

4-Aminobenzoic acid (*para*-aminobenzoic acid, 4ABA) is commonly used as a model system for the exploration of solvent-mediated proton transfer at the molecular level¹⁻³ because it has two different protonation sites: one on the amine group (*N*-protomer) and the other on the carboxylic group (*O*-protomer). The relative energies of these isomers are solvent dependent such that the *N*-protomer is more stable in solution by ~20 kJ/mol⁴⁻⁷ whereas the *O*-protomer is energetically favored by 30-40 kJ/mol in isolation (i.e. the gas phase). Survey calculations of the two isomers hydrated with $n = 1-3$ water molecules at the CCSD(T)/Def2-TZVPP level of theory carried out in this study (*vide infra*, **Fig. 1**) show that the relative energies decrease with incremental hydration of protonated 4ABA (hereafter denoted H⁺4ABA). Similar behavior for the microhydration of the analogous protomers of benzocaine was also reported recently.⁸

The higher energy *N*-protomer can be generated in the gas phase by kinetically trapping it using electrospray ionization (ESI) with an aprotic solvent (commonly acetonitrile, ACN).^{6, 7, 9-13} This raises the possibility that subsequent complexation with a protic solvent can drive the system toward the *O*-protomer.^{2, 4-7, 12, 14, 15} Using this property, several recent reports have characterized the *O*-protomer of H⁺4ABA·(H₂O)_{*n*} [hereafter denoted H⁺O·(H₂O)_{*n*}] with vibrational spectroscopy in the mid-IR region^{1, 7} and ion mobility measurements.² Based on these results,

it was proposed that protic solvent molecules are involved in the proton transfer process from the amino to the carboxylic group.^{1, 2} However, because H⁺4ABA hydration was carried out on ions generated in the ESI source region,^{1, 2, 7} as is typical in microhydration studies,^{16, 17} the presence of H₂O complicates the generation and subsequent characterization of the hydrated *N*-protomer (hereafter denoted H⁺N·(H₂O)_{*n*}). This complication can be overcome by hydrating H⁺N ions after they have been generated and isolated at low pressure in a radiofrequency ion trap, a scheme that has been demonstrated by the Garand group on various peptides for subsequent structural characterization using cryogenic ion vibrational spectroscopy.^{18, 19} This approach involves the integration of two ion traps. The first is held at 80 K (denoted the LN₂ trap) in which H₂O molecules are condensed onto the bare ions and cooled. These ions are then passed into a

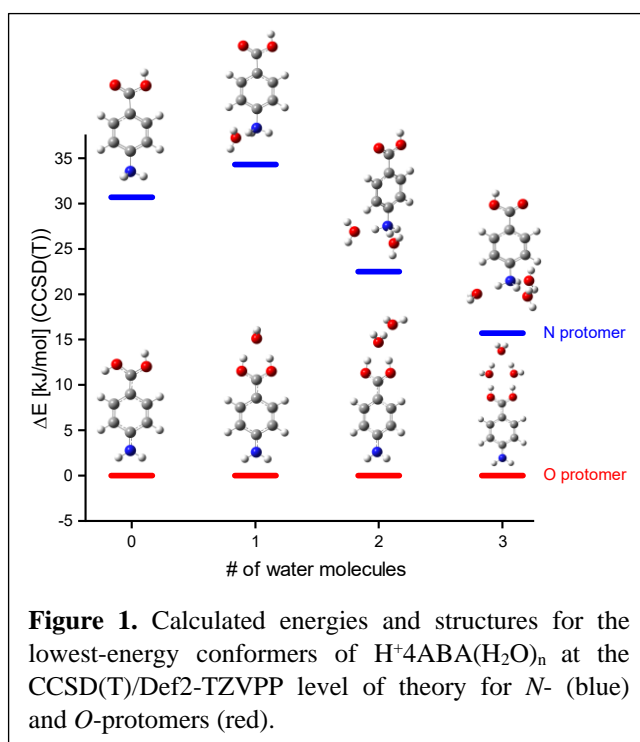


Figure 1. Calculated energies and structures for the lowest-energy conformers of H⁺4ABA(H₂O)_{*n*} at the CCSD(T)/Def2-TZVPP level of theory for *N*- (blue) and *O*-protomers (red).

second, 20 K cryogenic ion trap for the condensation of weakly bound D_2 molecules to enable vibrational spectroscopy by IR photodissociation (IRPD).²⁰ In this paper, we exploit this method to investigate the structures of the cold clusters that are formed by condensation of H_2O onto the *N*-protomer of the 4ABA scaffold in which all four labile protons are replaced by D (i.e., $(ND_3C_6H_4COOD)^+$, hereafter denoted D^+N). This arrangement allows us to determine the extent to which condensation triggers conversion to the *O*-protomer as well as the extent of H/D chemical exchange. In the event that the latter occurs, it is of interest to ascertain which deuterons on the D^+ABA scaffold participate in chemical exchange.

II. Experimental and computational details

More details for the experimental methods are available in **Section S1** of the *Supporting Information*. Briefly, an acidified (pH = ~2) 1 mM solution of 4ABA (1:9 D_2O :ACN) underwent electrospray ionization (ESI), generating ions that were then transported to the LN_2 trap held at 80 K using octopole radiofrequency (RF) ion guides. In the LN_2 trap, He buffer gas doped with a small amount of H_2O (<1%) was used to condense H_2O on the ions. The resulting hydrated clusters were then extracted and re-trapped in a 3D Paul trap held at 20 K, where they were further cooled and “tagged” with D_2 . These tagged ions were then transferred to a double-focusing time-of-flight photofragmentation mass spectrometer. IR spectra were obtained with a tunable OPO/OPA laser (LaserVision) over the range 800-4000 cm^{-1} . The present instrument configuration is presented in reference 21.

Minimum energy structures and harmonic spectra for various $H^+4ABA \cdot (H_2O)_{n=0-3}$ isomers were calculated at the CAM-B3LYP+D3/Def2-TZVPP level of theory using the Gaussian 16 program package.²² The energies of a few selected structures (see details in **Section S2**) were refined at the CCSD(T)/Def2-TZVPP level of theory. The energies of the various $H^+4ABA \cdot (H_2O)_{n=0-3}$ isomers are summarized in **Table S1-S5** with their corresponding structures shown in **Figure S1-S4**. Although the lowest detailed configurations of the floppy water clusters lie close in energy and vary with the method of the electronic structure calculation, the *O*-protomer isomers are significantly lower in energy than the *N*-protomer isomers for the first three hydrates with the trend indicated in **Figure 1**.

III. Results and discussion

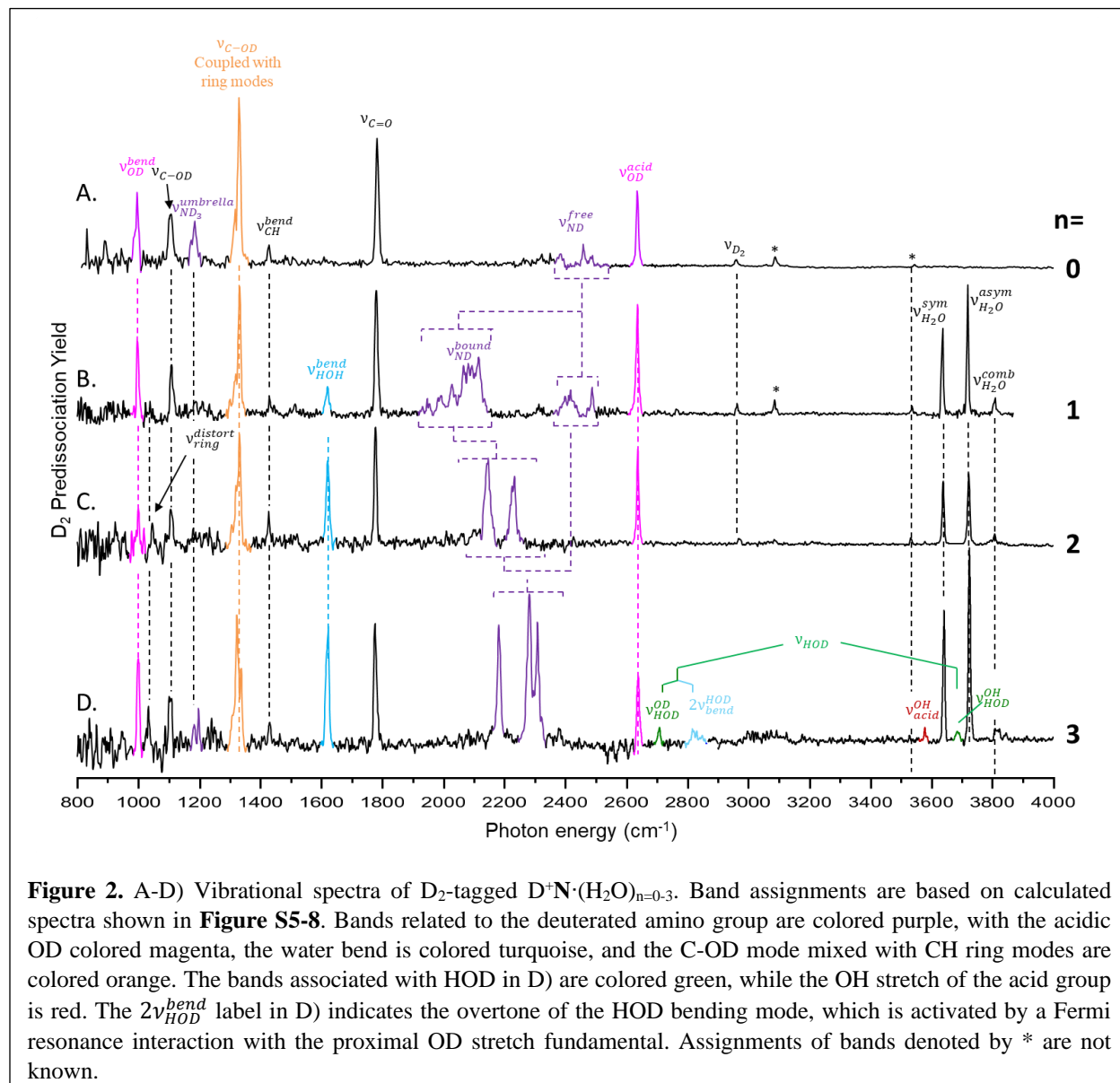


Figure 2 displays the D₂-tagged vibrational spectra of the D⁺N·(H₂O)_{n=0-3} clusters in which all four labile H atoms in the 4ABA scaffold are replaced by D. The three spectral markers for the acidic motif unique to the *N*-protomer are colored magenta and orange in **Figure 2A**. These are the OD stretch (ν_{OD}^{acid}), bend (ν_{OD}^{bend}), and C-OD stretch (ν_{C-OD}) at 2636, 996, and 1330 cm⁻¹, respectively. The unique carbonyl stretch, $\nu_{C=O}$, at 1791 cm⁻¹ is the telltale feature showing that the *N*-protomer is indeed the dominant species in all three hydrates. Note that the carboxylic acid group does not participate in hydrogen bonding in the hydrates since the acidic OD stretch is unperturbed in the three spectra. The various bands in the observed spectra of the hydrates are assigned based on calculated spectra, which are

shown in **Figure S5-S8**. Features associated with the water molecules are remarkably simple: bands that appear highest in energy arise from the symmetric ($\nu_{H_2O}^{sym}$) and antisymmetric ($\nu_{H_2O}^{asym}$) stretch fundamentals of water molecules docking in a single H-bond acceptor motif.²³ As such, it is immediately evident that, as expected,¹ the first three water molecules do not interact with one another and attach to the three hydrons in the ND_3^+ head group. This docking motif is consistent with the minimum energy structures indicated in **Figure 1**, and has been observed previously in the analogous hydrated anilinium,¹ ammonium,²⁴ and various protonated amino acids.^{18, 19, 25, 26} The three features associated with the tethered H_2O molecules ($\nu_{H_2O}^{sym}$, $\nu_{H_2O}^{asym}$, and ν_{HOH}^{bend}) provide clear evidence that when condensed onto the D^+N ion, most of the water molecules remain intact (do not undergo H/D exchange with the core ion). This observation is consistent with previous results reported by Garand and coworkers.^{18, 19}

The features associated with the amino headgroup (colored purple in **Fig. 2**) signal formation of the first hydration shell by donating H-bonds to each water molecule. Perhaps the most dramatic change going from $n = 0$ to $n = 1$ is the $\sim 400\text{ cm}^{-1}$ red shift of the $ND\text{---}OH_2$ stretch (ν_{ND}^{bound}) from the free ND stretching region of $\sim 2500\text{ cm}^{-1}$ to $\sim 2100\text{ cm}^{-1}$ in **Figure 2B**. The complex multiplet structure that spans $\sim 400\text{ cm}^{-1}$ of this ν_{ND}^{bound} band is typical of strong H-bonds,¹⁷ which often reflects a combination of Fermi resonance interactions with the bend overtone as well as activation of combination bands with soft modes.^{27, 28} Going from $n = 1$ to $n = 3$, the ν_{ND}^{bound} band is blueshifted steadily as each of the ND groups attaches a water molecule to complete the first hydration shell. This solvatochromic blue shift is a statement of the anticooperative behavior of multiple H-bonds.²⁹⁻³² Here, the additional H-bond formed between the amino headgroup and a second water molecule weakens the first H-bond already in play with the first water molecule. The asymmetric triplet structure of the ND stretches in the $n = 3$ spectrum is simplest with the lowest band at 2181 cm^{-1} arising from the non-degenerate ND_3 symmetric stretch while the upper doublet centered at 2298 cm^{-1} arises from the ($\sim 30\text{ cm}^{-1}$) splitting of the antisymmetric stretch due to the reduced symmetry of the amino group by the proximal benzene ring. This pattern is recovered at the harmonic level as displayed by the calculated spectrum for $n = 3$ in **Figure S8B**.

For the $n = 0-2$ hydrates, some weak, unassigned peaks are observed in the NH/OH stretching region. The feature at 3085 cm^{-1} , for instance, appeared most strongly for the $n = 0$ and 1. This peak was also observed for the bare, non-deuterated ion reported previously,⁷ hence is likely an overtone or a combination band. A small peak is observed at 3530 cm^{-1} for the entire hydrated series. This peak is close to the bend-stretch combination band of ammonia,^{33, 34} shifted upon deuteration, but since it is observed throughout the hydration series, it is not an NH/OH feature. Lastly, the peak at 3808 cm^{-1} is the combination band of low frequency torsional modes with the $\nu_{H_2O}^{asym}$,^{35, 36} which has been observed for

various water cluster systems.^{37, 38} Hence, there is no trace of the OH and OD bands associated with the formation of HOD, establishing that no chemical exchange occurs in the small systems.

For the $n = 3$ cluster, however, there are spectral features of the HOD moiety in the spectrum of the $n = 3$ complex presented in **Figure 2D**. Specifically, the OH stretch of the HOD (ν_{HOD}^{OH}) occurs between the $\nu_{H_2O}^{sym}$ and $\nu_{H_2O}^{asym}$ water modes at 3686 cm^{-1} and its associated OD stretch (ν_{HOD}^{OD}) is also evident at 2707 cm^{-1} (both colored green). An additional band is also observed at 2820 cm^{-1} (turquoise) that is close to the location of the bend overtone of HOD. The $\nu = 2$ level of the bend is known to undergo a strong Fermi-type interaction with the OD $\nu = 1$ level with a matrix element of about 40 cm^{-1} .³⁹ The onset of H/D exchange was also confirmed by following the collision-induced fragmentation of the $D^+N\cdot(H_2O)_n$ clusters with the results presented in **Figure S9**. This study revealed that the $n = 1$ and 2 clusters only fragment with loss of $m/z = 18$, whereas clusters with $n \geq 3$ are observed to eject both $m/z = 18$ and 19. Together, these results establish that chemical exchange of hydrons on the N -protomer 4ABA scaffold can occur without formation of the O -protomer.

The observation of H/D exchange raises the question of which of the four hydrons in the 4ABA scaffold is participating in this process. Interestingly, there is a small peak that corresponds to the acid OH (ν_{acid}^{OH} , red) at 3574 cm^{-1} ,⁷ suggesting a mechanism wherein the exchange occurs at the more acidic -COOD functionality rather than at the location of positive charge concentration at the $-ND_3^+$ group. A comparison of the D/H $^+N\cdot(H_2O)_3$ spectra are shown in **Figure S10A-B**. The ν_{acid}^{OH} is observed in both D/H spectra, while the sharp N-H modes are only observed for the H $^+N\cdot(H_2O)_3$. Moreover, since the spectra displayed in **Figure 2** correspond to the ions quenched to $\sim 20\text{ K}$, exchange at the acid site does not yield the O -protomer. If the O -protomer were present, for example, the intense series of peaks from $1500\text{-}1700\text{ cm}^{-1}$, shown in **Figure S10C**, would have been detected. Our experimental spectra, on the other hand, only shows the ν_{HOH}^{bend} for the H $^+N\cdot(H_2O)_3$ spectrum in **Figure 2C**. This behavior also indicates that H/D exchange occurred prior to heating in the CID measurements yielding HOD loss as discussed above.

IV. Summary

We have demonstrated trapping of the metastable N -protomer of 4ABA and its complexes with three water molecules by analysis of the vibrational band patterns using IR photodissociation of the D₂ tagged species. This is accomplished using two cold ion traps, one to condense water molecules and the second to form the D₂ adducts required for the application of predissociation spectroscopy. The first three water molecules attach to the three hydrons in the N -protomer, demonstrating that the barrier for formation of the more stable O -protomers is not efficiently overcome by the condensation energy of water

molecules onto the *N*-protomer. No isotope scrambling is observed in the $n = 1$ and 2 clusters, but is observed for $n = 3$ as evidenced both by the presence of the telltale HOD stretching bands in the vibrational spectrum and the loss of $m/z = 19$ upon collisional dissociation in the trap. Upon scrambling, the acidic OH group is observed to undergo H/D exchange for $n = 3$ without formation of the *O*-protomer.

SUPPLEMENTARY MATERIAL

See the Supplementary Material for detailed descriptions of the experimental and computational details and results.

ACKNOWLEDGEMENTS

M.A.J gratefully acknowledges the Department of Energy through the condensed phase and interfacial molecular science (CPIMS) program under Grant DE-SC0021012 for support of this work. T.K. thanks the National Institutes of Health for stipend support provided under Biophysical Training Grant No. 5T32GM008283-32. K.G. thanks the Fonds National de la Recherche, Luxembourg, for funding the project GlycoCat (13549747) and the Fulbright Program for funding his research stay at Yale University.

AUTHOR DECLARATIONS

Conflict of Interest

The authors have no conflicts to disclose.

DATA AVAILABILITY

The data that support the findings of this study are available from the corresponding author upon reasonable request.

References

- ¹T. M. Chang *et al.*, *J Am Chem Soc* **134** (2012) 15805.
- ²M. J. Hebert, and D. H. Russell, *J Phys Chem B* **124** (2020) 2081.
- ³P. R. Batista *et al.*, *Phys Chem Chem Phys* **23** (2021) 19659.
- ⁴X. X. Zhang *et al.*, *J Phys Chem B* **104** (2000) 8598.
- ⁵Z. X. Tian, and S. R. Kass, *Angewandte Chemie-International Edition* **48** (2009) 1321.
- ⁶J. Seo *et al.*, *Phys Chem Chem Phys* **18** (2016) 25474.
- ⁷T. Khuu, N. Yang, and M. A. Johnson, *International Journal of Mass Spectrometry* **457** (2020)
- ⁸K. Hirata *et al.*, *Phys Chem Chem Phys* **24** (2022) 5774.
- ⁹Z. Tian, and S. R. Kass, *Angew Chem Int Ed Engl* **48** (2009) 1321.
- ¹⁰J. Schmidt *et al.*, *Journal of Physical Chemistry A* **115** (2011) 7625.
- ¹¹J. L. Campbell, J. C. Y. Le Blanc, and B. B. Schneider, *Analytical Chemistry* **84** (2012) 7857.
- ¹²A. P. Cismesia, G. R. Nicholls, and N. C. Polfer, *Journal of Molecular Spectroscopy* **332** (2017) 79.
- ¹³A. L. Patrick *et al.*, *International Journal of Mass Spectrometry* **418** (2017) 148.
- ¹⁴B. Ucur *et al.*, *Journal of the American Society for Mass Spectrometry* (2022)
- ¹⁵H. X. Xia, and A. B. Attygalle, *J Mass Spectrom* **53** (2018) 353.

- ¹⁶ N. Yang *et al.*, P. Natl. Acad. Sci. USA **117** (2020) 26047.
- ¹⁷ S. Mitra *et al.*, The Journal of Physical Chemistry A **126** (2022) 1640.
- ¹⁸ J. M. Voss, K. C. Fischer, and E. Garand, Journal of Physical Chemistry Letters **9** (2018) 2246.
- ¹⁹ K. C. Fischer *et al.*, Journal of Physical Chemistry A **123** (2019) 3355.
- ²⁰ S. J. Stropoli *et al.*, Journal of Chemical Physics **156** (2022)
- ²¹ S. J. Stropoli *et al.*, The Journal of Physical Chemistry Letters **13** (2022) 2750.
- ²² M. J. Frisch *et al.*, Wallingford, CT, 2016).
- ²³ N. Yang *et al.*, J. Phys. Chem. A **124** (2020) 10393.
- ²⁴ Y.-S. Wang *et al.*, J. Am. Chem. Soc. **120** (1998) 8777.
- ²⁵ A. Kamariotis *et al.*, J Am Chem Soc **128** (2006) 905.
- ²⁶ H. Wincel, Chemical Physics Letters **439** (2007) 157.
- ²⁷ A. B. McCoy, Journal of Physical Chemistry B **118** (2014) 8286.
- ²⁸ H. J. Zeng *et al.*, Journal of Physical Chemistry A **124** (2020) 10507.
- ²⁹ R. Ludwig, Phys. Chem. Chem. Phys. **4** (2002) 5481.
- ³⁰ L. Albrecht, S. Chowdhury, and R. J. Boyd, J. Phys. Chem. A **117** (2013) 10790.
- ³¹ J. M. Guevara-Vela *et al.*, Phys. Chem. Chem. Phys. **18** (2016) 19557.
- ³² S. G. Olesen *et al.*, Chem. Phys. Lett. **509** (2011) 89.
- ³³ E. Salli, T. Salmi, and L. Halonen, Journal of Physical Chemistry A **115** (2011) 11594.
- ³⁴ N. W. Cant, and L. H. Little, Can J Chemistry **45** (1967) 3055.
- ³⁵ G. E. Douberly *et al.*, J. Phys. Chem. A **114** (2010) 4570.
- ³⁶ D. C. McDonald *et al.*, The Journal of Physical Chemistry Letters **9** (2018) 5664.
- ³⁷ N. Heine *et al.*, J. Am. Chem. Soc. **135** (2013) 8266.
- ³⁸ L. I. Yeh *et al.*, J. Chem. Phys. **91** (1989) 7319.
- ³⁹ W. S. Benedict, N. Gailar, and E. K. Plyler, J. Chem. Phys. **24** (1956) 1139.